Structural, Optical, and Photovoltaic Properties of Ni-Doped CdZnS Nanoparticles: A Comparative Study

Faruk DEMIR*
*Department of Electrical and Electronic Engineering, Siirt University, Siirt, TURKEY

ABSTRACT

Un-doped and Ni (5%, 7.5% and 10%) doped CdZnS nanoparticles (NPs) were prepared by the co-precipitation method at room temperature using the mercaptoethanol as a capping agent. J-V measurements were carried out for Ni-doped CdZnS NPs for the first time in this study, showed that Ni-doped CdZnS NPs can be utilized as sensitizers to improve the performance of solar cells. In addition to the photovoltaic properties, structural and optical properties of Ni-doped CdZnS NPs have been investigated. Study (XRD) on the structural properties showed that un-doped and Ni-doped CdZnS NPs have cubic (zinc blende) structure and the particle size of doped CdZnS NPs becomes smaller than un-doped CdZnS NPs. Optical absorption revealed that the absorption of Ni-doped CdZnS is blue shifted compare to un-doped CdZnS NPs. Consequently, the results indicate that Ni-doped CdZnS NPs can be suitable material for photovoltaic applications

KEYWORDS: co-precipitation; doping; nanoparticles; photovoltaic; semiconductors.

I. INTRODUCTION

CdS and ZnS which have band gap of 2.42 and 3.6 eV at room temperature are important members of II-VI semiconductors. CdZnS, which has a wider band gap than CdS, increases short circuit current in solar cell devices. The CdZnS is a capable material for opto-electronic applications in UV-VIS spectral region owing to its wide band gap features. It has also been reported that lattice constant of CdZnS which is suitable for electronic device manufacturing, is well matched to common substrates such as GaAs and Si [1-3].

From the application point of view, CdS and ZnS NPs doped with transition metals have been studied as an alternative strategy to boost the efficiency of solar cells because they create long–lived photogenerated charge carriers, reduce the electron-hole recombination, and have a long lifetime and facilitate the charge transfer from the NPs to the photoelectrode [4-9]. Gopi et al. [10] reported that CdNiS cell exhibits the best photovoltaic performance with power conversion efficiency (η) of 3.11%. However, no work was found about solar cell application of Ni-doped CdZnS NPs. For this reason, this study will be original.

In our present study, the effect of Ni content on the photovoltaic properties of CdZnS NPs is discussed for the first time. The synthesis and characterization of un-doped and Ni (5%, 7.5% and 10%) doped CdZnS NPs have been reported, prepared by the co-precipitation method at room temperature using the mercaptoethanol as a capping agent. Their structural, optical and photovoltaic properties have been studied.

II. EXPERIMENTAL DETAILS

Commercial $Cd(CH_3COO)_2.2H_2O$ as Cd source, Zn $(CH_3COO).{}_2H_2O$ as Zn source, Ni $(NO_3)_2{\bullet}6H_2O$ as Ni source, and Na_2S as S source, were of analytical grade and were used without further purification to synthesize un-doped and Ni (5%, 7.5% and 10%) doped CdZnS NPs at room temperature using co-precipitation method. Mercaptoethanol (C_2H_6OS) was used as a capping agent to prevent any agglomeration during the preparation.
For synthesis of un-doped CdZnS; 0.5 M aqueous solutions of $Cd(CH_3COO)_2.2H_2O$, 0.025 M aqueous solutions of Zn $(CH_3COO).{}_2H_2O$ and 0.5 M aqueous solutions of Na_2S were dissolved into three different beakers. These three solutions cation and anion sources were transferred into fourth clean beaker and stirred at certain time to get homogeneous mixture of CdZnS at room temperature. While stirring, the mercaptoethanol (2 ml) was added onto the mixture. The precipitated sample was separated from the solution by a filter paper. De-ionized water and ethanol were used to wash the resultant particles to get rid of unwanted compounds inside the particles. The obtained final solution was heated in oven at 80 ^{0}C. Orange color of CdZnS NPs was obtained after grinding the powders using a mortar.

For synthesis of Ni (5%, 7.5% and 10%) doped CdZnS NPs; 0.025 M, 0.0375 M and 0.05 M aqueous solutions of Ni $(NO_3)_2{\bullet}6H_2O$ were added onto the solution of [0.5 M $Cd(CH_3COO)_2.2H_2O$ and 0.025 M Zn $(CH_3COO).{}_2H_2O$], separately then, followed the same procedure as mentioned above.

X-ray diffraction (XRD) on a Rigaku x-ray diffractometer with Cu K_α (λ= 154.059 pm) [11] radiation were used to characterize the structural properties of the samples. UV-VIS absorption spectra were recorded using a Perkin-Elmer Lambda 2 [12] spectrometer. Photoluminescence (PL) measurement was carried out with a Perkin-Elmer LS 50B [13] at room temperature, using 310 nm as the excitation wavelength. The magnetic properties of un-doped and Ni (5%, 7.5% and 10%) doped CdZnS NPs were analyzed using a physical property measurement system (PPMS) [14]. Current densities (J) versus voltage (V) measurements were performed by using PEC-S20 with a monochromatic light source consisting of a 150-W Xe lamp and a monochromator [15]. For J-V measurements, fluorine doped tin oxide (FTO, 13Ω.sq^{-2}) conductive glass substrates were used as the photo electrodes. The TiO_2 paste were coated on the FTO substrates using the doctor blade method, and then sintered at 450 0C for 45 minutes. A suspension of un-doped and Ni (5%, 7.5% and 10%) doped CdZnS NPs were dropped on the FTO substrates with the TiO_2 paste. The substrates were dried with N_2 gas and secured against Cu_2S counter electrodes containing polysulfide electrolytes.

III. RESULTS AND DISCUSSIONS

The XRD patterns of un-doped and Ni (5%, 7.5% and 10%) doped CdZnS NPs are indicated in Fig. 1. It can be clearly seen that all the diffraction peaks of NPs can be well indexed as the zinc blende (cubic) phase structure of CdS, which are consistent with the standard card (JCPD No: 65-2887). It was observed that the three diffraction peaks correspond to the lattice planes of (111), (220) and (311), respectively, suggesting that Ni contents have been incorporated into the CdZnS lattice. The XRD patterns demonstrate that the full width at half height maximum (FWHM) of the diffraction peaks increases with doping concentration which results in the degradation and decrease in the crystalline size. Based on the FWHM, the average particle sizes (*PS*s) of un-doped and Ni-doped CdZnS NPs, were calculated using the Debye-Scherrer equation, $PS=0.9\lambda/(\beta cos\theta)$; where λ=0.15418 nm, is the x-ray wavelength provided from a Cu (α) radiation, β is the FWHM in radians and θ is the Bragg's angle, are 2.56 , 2.48, 2.43 and 2.39 nm, respectively. The Ni^{2+} ions occupy the regular lattice site of Cd^{2+} ions that what may be possible reason for the decrease in the crystalline size. Moreover, this ion substitution could cause the crystal defects and charge imbalance in CdZnS structure.

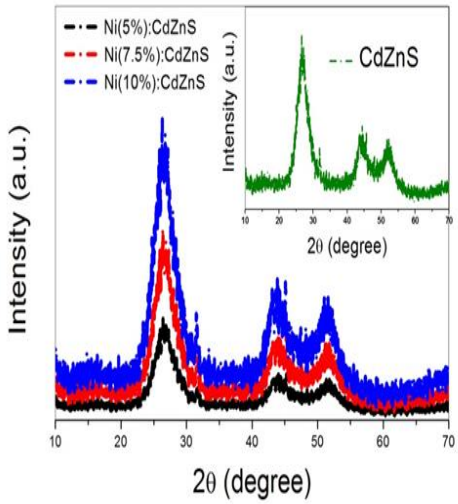

Fig.1 X-ray diffraction patterns of un-doped CdZnS (inset) and Ni (5%, 7.5% and 10%) doped CdZnS NPs.

We investigated the optical properties and analyzed the band gap of un-doped and Ni-doped CdZnS NPs by UV-visible absorption spectroscopy. Crystal imperfection may occur due to the dopant which changes the band gap of semiconductor. Figure 2 reveals the optical absorption spectra for un-doped and Ni-doped CdZnS NPs in the wavelength range 300–800 nm. Some factors such as particle size and defects in the structure can change the absorbance of the samples. The UV-VIS absorption spectra show the ultraviolet cut-off absorption of Ni- doped CdZnS shifts to higher energy (shorter wavelength) compared with un-doped CdZnS. The absorption edge is found to shift towards shorter wavelengths (blue shift) which mean the band gap increases which may be caused by crystallite size as the doping concentrations increase.

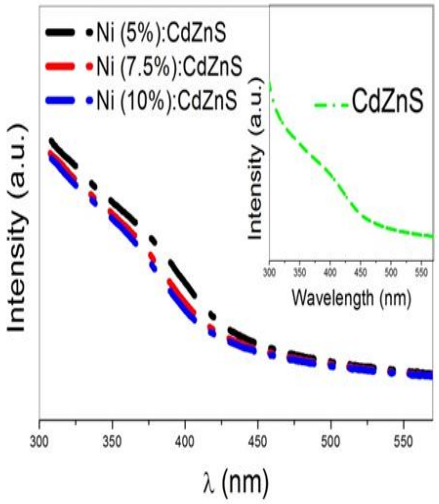

Fig. 2 UV-VIS absorption spectrums of un-doped CdZnS (inset) and Ni (5%, 7.5% and 10%) doped CdZnS NPs.

The Tauc relation [16] is given in Equation 1, were used to calculate the energy band gap (E_g) of the NPs.

$\alpha h\upsilon = C(h\upsilon - E_g)^n$ (1)

Where α is the absorption coefficient, n=1/2 or 2 for direct or indirect allowed transition, respectively, C is the characteristic parameter for respective transitions, hυ is photon energy and E_g is energy band gap. Plots of $(\alpha h\upsilon)^2$ versus hυ for un-doped and Ni (5%, 7.5% and 10%) doped CdZnS NPs are shown in Fig.3.

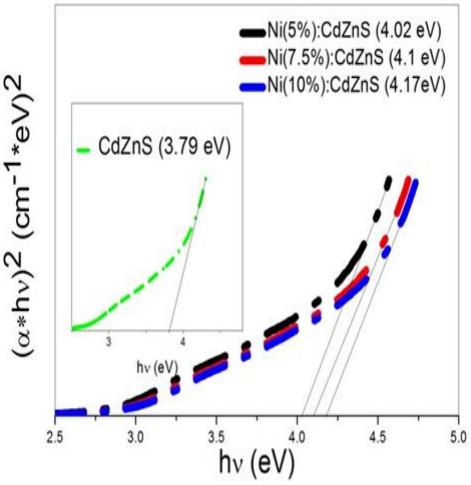

Fig.3 Determination of the optical band gap of un-doped CdZnS (inset) and Ni (5%, 7.5% and 10%) doped CdZnS NPs using $(\alpha h\upsilon)^2$ vs. hυ plot.

As can be seen in Fig. 3, the un-doped CdZnS has a large band gap (3.79 eV) which increases with increasing in the Ni concentration. The blue shift in the absorption edge is due to the quantum confinement of the excitons present in the sample, causing more discrete energy spectrum of the individual NPs. Using Brus's equation is given in ref [17], the particle sizes for un-doped and Ni (5%, 7.5% and 10%) doped CdZnS NPs were calculated. Table 1 indicates the band gap and size calculation for samples.

Table 1 Particle size and band-gap variation with Ni concentration.

Sample (NPs)	Band gap energy (eV)	Particle size (nm)
Un-doped CdZnS	3.79	2.40
Ni (5%) doped CdZnS	4.02	2.24
Ni (7.5%) doped CdZnS	4.1	2.19
Ni (10%) doped CdZnS	4.17	2.16

It was found that Ni content results in the reduction in size of CdZnS NPs which clearly relates with increasing in the band gap value. The reason of this could be due to the quantum confinement effect on the bulk of CdS. The effect of the quantum confinement on impurity depends upon the size of the host crystal. The obtained sizes for un-doped and Ni (5%, 7.5% and 10%) doped CdZnS NPs are in good agreement with the results from XRD analysis.

The optical properties of NPs are explored by photoluminescence (PL) which is a perceptive helpful method [18]. It gives us information about the energy states of impurities and defects, yet at very low densities, for understanding structural defects, the crystallinity, surface defects, energy bands and exciton fine structure. The defects like sulfur vacancies in grain boundaries and the presence of doping atoms in the surface and intergranular layers which affect some physical properties such as optical properties of nano sized metal sulfide materials [19]. Fig. 4 demonstrates the room temperature PL excited with a wavelength of 310 nm for un-doped and Ni (5%, 7.5% and 10%) doped CdZnS NPs in the wavelength range 492-800 nm. It is seen that the un-doped CdZnS NPs has only one green emission band centered at 510.7 nm, which is related to radiative recombination involving defect states in the CdZnS NPs. The emission peaks at 575.6, 582.2 and 592.5 nm which correspond to *d-d* transition between Ni ions, are observed for Ni (5%), Ni (7.5%) and Ni (10%) doped CdZnS NPs, respectively. In case of higher Ni concentrations, the emission peaks of Ni doped CdZnS NPs are red-shifted. This red-shift could be due to the strong *p-d* hybridization and quantum confinement effect of NiS cluster in CdZnS NPs [20].

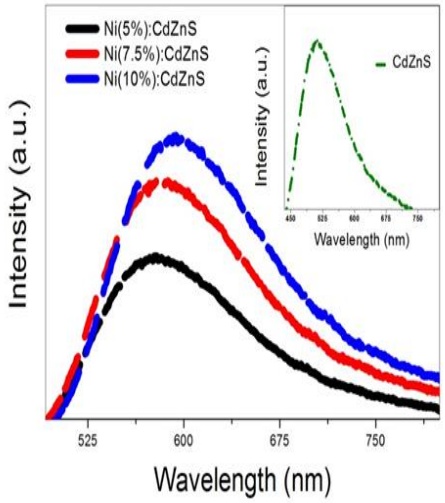

Fig.4 Photoluminescence (PL) spectra at room temperature excited with a wavelength of 310 nm (4.0 eV) for un-doped CdZnS (inset) and Ni (5%, 7.5% and 10%) doped CdZnS NPs.

The plot of current density (J) versus voltage (V) for the un-doped CdZnS and Ni (5%, 7.5% and 10%) doped CdZnS NPs is shown in Fig.5. The samples were examined under 100 mW/cm^2 light intensity.

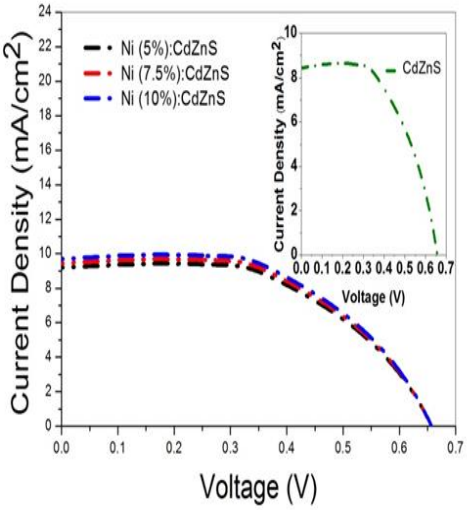

Fig. 5 J-V plots for un-doped CdZnS (inset) and Ni (5%, 7.5% and 10%) doped CdZnS NPs.

It is important to note that there is a significant improvement in the performance CdZnS NPs with increase in Ni concentration. Table 2 indicates the power conversion efficiencies were found 2.67, 2.88, 2.95 and 3.05 for un-doped and Ni (5%, 7.5% and 10%) doped CdZnS NPs, respectively.

Table 2 Values of J_{SC}, V_{OC}, η % for un-doped CdZnS and Ni (5%, 7.5% and 10%) doped CdZnS NPs, respectively.

Samples (NPs)	Short Circuit Current Density, J_{SC}, (mA/cm^2)	Open Circuit Voltage, $V_{OC,}$ (V)	Power conversion efficiency (η %)
CdZnS	8.36	0.68	2.67
Ni(5%):CdZnS	9.21	0.66	2.88
Ni(7.5%):CdZnS	9.47	0.66	2.95
Ni (10%):CdZnS	9.8	0.66	3.05

As can be seen clearly from the Table 2, there is a significant improvement in the performance of the CdZnS NPs when they are doped with different concentrations of Ni. The effect of Ni content on the performance of the CdZnS can be explained that owing to Ni doping, the contact between CdZnS NPs and TiO_2 NW becomes good. Thus, this contact can block the interfacial recombination of the injected transfer from NWs to polysulfide electrolytes. Correspondingly, it improves the performance of the devices made from CdZnS NPs [21]. Another reason can be explained that the CdZnS NPs doped with Ni passivation reduce the recombination processes at the surface of NPs.

IV. CONCLUSIONS

In this study, the structural, optical, photovoltaic and magnetic properties of un-doped and Ni (5%, 7.5% and 10%) doped CdZnS NPs, prepared by the co-precipitation method at room temperature using the mercaptoethanol as a capping agent, were investigated. Study (XRD) on the structural properties showed that un-doped and Ni (5%, 7.5% and 10%) doped CdZnS NPs have cubic (zinc blende) structure and the particle size of CdZnS NPs doped by Ni becomes smaller than un-doped CdZnS NPs. The optical absorption spectra revealed that the absorbance of Ni (5%, 7.5% and 10%) doped CdZnS NPs are blue shifted compare to un-doped CdZnS NPs. It means that the band gap increases which may be caused by crystallite size as the doping concentrations increase. It was also observed the enhancement in PL intensities may be ascribed to the creation of new radiation centers or size reduction caused by Ni doping in CdZnS matrix. J-V measurements were carried out for Ni (5%, 7.5% and 10%) doped CdZnS NPs for the first time in this study, showed that Ni (5%, 7.5% and 10%) doped CdZnS NPs can be utilized as sensitizers to improve the performance of solar cells. The power conversion efficiency (η %) was obtained as 2.67, 2.88, 2.95 and 3.05 for un-doped and Ni (5%, 7.5% and 10%) doped CdZnS NPs, respectively. Consequently, the results indicate that Ni (5%, 7.5%, and 10%) doped CdZnS NPs can be suitable materials for photovoltaic applications.

V. REFERENCES

[1] T. Yamamoto, S. Kishimoto, S. Ilida, "Control of valence states for ZnS by triple-co doping method", Physica B: Condensed Matter, 308, 916-919, 2001.

[2] A. A. Khrosravi, F. B. Bigdeli, M. Yousefi, M. S. Abdikhani, S. M. T. Otaqsara, "Nickel and manganese-doped CdS quantum dots: Optical study and photocatalytic activity on methylene blue", Environmental Progress & Sustainable Energy, 33, 1194-1200, 2014.

[3] A. M. Salem, "Structure, refractive-index dispersion and the optical absorption edge of chemically deposited ZnxCd(1-x)S thin films", Applied Physics A, 74, 205-211, 2002.

[4] S. Horoz, Q. Dai, F. S. Maloney, B. Yakami, J. M. Pikal, X. Zhang, J. Wang, W. Wang, J. Tang, "Absorption Induced by Mn Doping of ZnS for Improved Sensitized Quantum-Dot Solar Cells", Physical Review Applied, 3, 024011, 2015.

[5] P. K.Santra, P. V. Kamat, "Mn-doped quantum dot sensitized solar cells: a strategy to boost efficiency over 5%", Journal of American Chemistry Society, 134, 2508-2511, 2012.

[6] Q. Dai, J. Chen, L. Liu, J. Tang, W. Wang, "Pulsed Laser Deposition of CdSe Quantum Dots on Zn2SnO4 Nanowires and Their Photovoltaic Applications", Nano Letters, 12, 4187-4193, 2012.

[7] S. Horoz, L. Liu, Q. Dai, B. Yakami, J. M. Pikal, W. Wang, J. Tang, "CdSe quantum dots synthesized by laser ablation in water and their photovoltaic applications", Applied Physics Letters, 101, 223902, 2012.

[8] S. Horoz, Q. Dai, U. Poudyal, B. Yakami, J. M. Pikal, W. Wang, J. Tang, "Controlled synthesis of Eu2+ and Eu3+ doped ZnS quantum dots and their photovoltaic and magnetic properties", AIP Advances, 6, 045119, 2016.

[9] S. Horoz, O. Sahin, "Investigations of structural, optical, and photovoltaic properties of Fe-alloyed ZnS quantum dots", Journal of Materials Science: Materials in Electronics, 28, 9559-9564, 2017.

[10] C. V. V. M. Gopi, M. V. Haritha, H. Seo, S. Singh, S. K. Kim, M. Shiratani, H. J. Kim, "Improving the performance of quantum dot sensitized solar cells through CdNiS quantum dots with reduced recombination and enhanced electron lifetime", Dalton Transactions, 45, 8447-8457, 2016.

[11] www.rigaku.com/en/products/xrd/smartlab

[12] http://www.geminibv.nl/labware/perkin-elmer-lambda-2-spectrofotometer-1/perkin-elmer-lambda-2-uv-vis-spectrometer-manual-eng.pdf/view

[13] http://www.perkinelmer.com/product/ls55-fluorescence-spectrophotometer-120v-l2250117

[14] https://www.qdusa.com/products/ppms.html

[15] [http://www.peccell.com/pdf/PEC-S20_E.pdf

[16] J. Tauc,"Amorphous and liquids semiconductors", Plenum Press, New York, 159, 1974.

[17] L. Brus, "Electronic wave functions in semiconductor clusters: experiment and theory", Journal of Physical Chemistry, 90, 2555-2560, 1986.

[18] M. H. Hassan, W. Khan, A. Azam, A. H. Naqvi, "Effect of size reduction on structural and optical properties of ZnO matrix due to successive doping of Fe ions", Journal of Luminescence, 145, 160-166, 2014.

[19] S. Shen, Q. Wang, "Rational Tuning the Optical Properties of Metal Sulfide Nanocrystals and Their Applications",Chemistry of Materials, 25, 1166-1178, 2013.

[20] A. Firdous, D. Singh, M. M. Ahmad, "Electrical and optical studies of pure and Ni-doped CdS quantum dots", Appliled Nanoscience, 3, 13-18, 2013.

[21] Y. Li, L. Wei, R. Zhang, Y. Chen, L. Mei, J. Jiao, "CdS quantum dot-sensitized solar cells based on nano-branched TiO2 arrays", Nanoscale Research Letters, 9, 107-115, 2013.